CHAPTER IV

RESULTS AND DISCUSSION

4.1 Finding the adsorption and decomposition efficiency and initial rate of titania in degrading phenol using the shaker-type photoreactor

A preliminary study of adsorption efficiency, decomposition efficiency, TOC depletion efficiency, and initial decomposition rate of titania nanoparticles in degrading phenol was necessary for the rotary drum filtering reactor design.

In this section, we defined the adsorption, decomposition, and depletion in TOC efficiencies as given in equations 4.1 - 4.6 (Viriya-empikul, 2004).

$$\text{Phenol-based adsorption efficiency (\%)} = (C_{b,NI}-C_{t,NI})/C_i \times 100 \qquad (4.1)$$

$$\text{Phenol-based total removal efficiency (\%)} = (C_{b,Ir}-C_{t,Ir})/C_i \times 100 \qquad (4.2)$$

$$\text{Decomposition efficiency (\%)} = \text{Phenol-based total removal efficiency (\%)} - \text{Phenol-based adsorption efficiency (\%)} \qquad (4.3)$$

$$\text{TOC-based adsorption efficiency (\%)} = (TOC_{b,NI}-TOC_{t,NI})/TOC_i \times 100 \qquad (4.4)$$

$$\text{TOC-based total removal efficiency (\%)} = (TOC_{b,Ir}-TOC_{t,Ir})/TOC_i \times 100 \qquad (4.5)$$

TOC depletion efficiency (%) = TOC-based total removal efficiency (%)

– TOC-based adsorption efficiency (%) (4.6)

The initial decomposition rate was calculated from equation 4.7 (Viriya-empikul, 2004). The initial concentration for this equation was the residual phenol concentration either after 10 min adsorption or after equilibrium adsorption.

$$\text{Initial decomposition rate} = (\Delta C)/(\Delta t) \quad (4.7)$$

Two titania with different crystallite sizes (see table 1.1) were used to investigate the photocatalytic activity and initial reaction rate of each titania in degrading phenol. The better photocatalyst would be chosen to treat the phenol solution in rotary drum filtering reactor system.

4.1.1 Phenol removal efficiency

Table 4.1 shows that the equilibrium time for dark adsorption of phenol by both titanias took less than 10 min. T1 had an adsorption capacity of about 4.21 % (5.83 mg g^{-1}) while N1, about 1.77 % (3.10 mg g^{-1}). Between the two titania, we considered that phenol molecules liked to adsorb on the surface of TiO_2 more than the apatite because the negative charges on the benzene ring are attracted to the positive charges on the surface of TiO_2. The decomposition efficiency of phenol and TOC depletion efficiency for 60 min by T1 were 19.72 and 14.86 %, respectively, while the decomposition efficiency of phenol and TOC depletion efficiency at this same time by N1 were 2.87 and 0.87 %, respectively. These results show that the decomposition efficiency of phenol by T1 was higher than N1 because the effective metal surface area of nano-sized T1 was higher than the micro-sized N1. As expected, depletion efficiency of intermediate product TOC by both titania was lower than the decomposition efficiency of the original reactant phenol. This implies that TOC was harder to remove than phenol because decomposition of phenol generally results in intermediate products that still contribute to TOC value.

Table 4.1 Phenol removal efficiency (%) and initial decomposition rate of each titania.

Code name	Average adsorption (without light source) (%)		Average decomposition by UV (excluding adsorption) (%)		TOC Depletion by UV (excluding adsorption) (%)		Initial decomposition rate (ppm min^{-1})
	10 min	60 min	10 min	60 min	10 min	60 min	
T1	4.21	4.67	0	19.72	0.85	14.86	$-r = 0.0179[C]$
N1	1.77	1.77	4.4	2.87	0.91	0.87	$-r = 0.0106[C]$

4.1.2 Initial rate of photocatalytic degradation

Both table 4.1 and Fig. 4.1 illustrate the initial reaction rate of each titania. The initial reaction rate of T1 in degrading phenol could be approximated as first-order reaction. T1 had the initial reaction rate constant of 0.0179 ppm min^{-1}. The fact that the TOC-based decomposition efficiency is always lower than the phenol-based efficiency indicates the formation of soluble byproducts such as catechol, benzoquinone and hydroquinone, which we have confirmed by HPLC analysis.

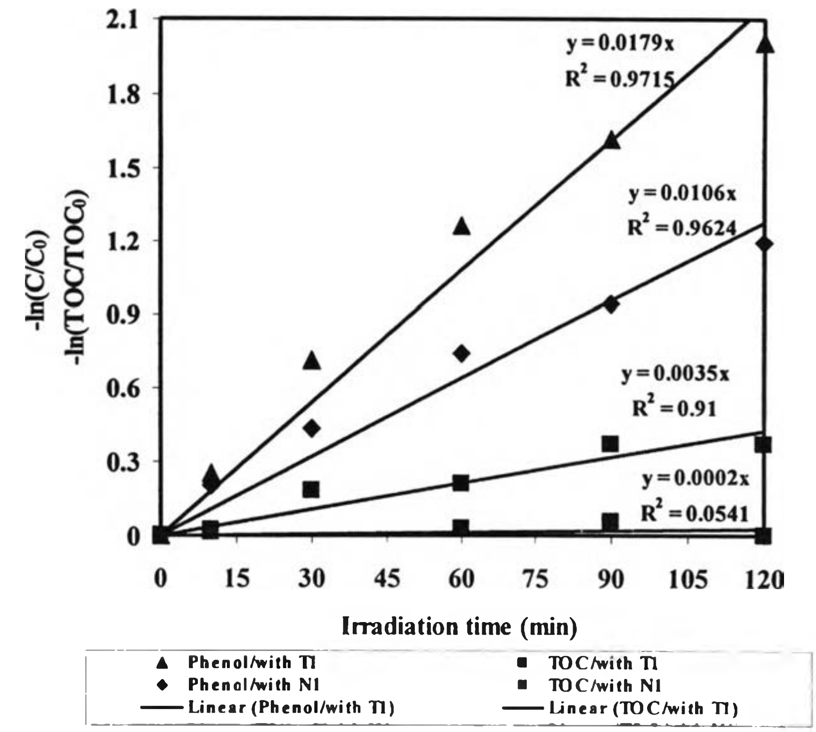

Figure 4.1. Comparison of phenol removal by each titania in terms of phenol and TOC.

T1 was more effective than N1 as photocatalyst and adsorbent so it was selected to treat the phenol solution in a rotary drum filtering reactor system.

4.2 Characterization of TiO_2 cake formed on the surface of HEPA filter

The SEM image of fibers of HEPA filter is shown in Fig. 4.2 while the SEM image of the TiO_2 (T1) cake formed on the surface of HEPA filter is shown in Fig. 4.3. This indicates that the TiO_2 nanoparticles are formed on the whole surface area of the HEPA filter.

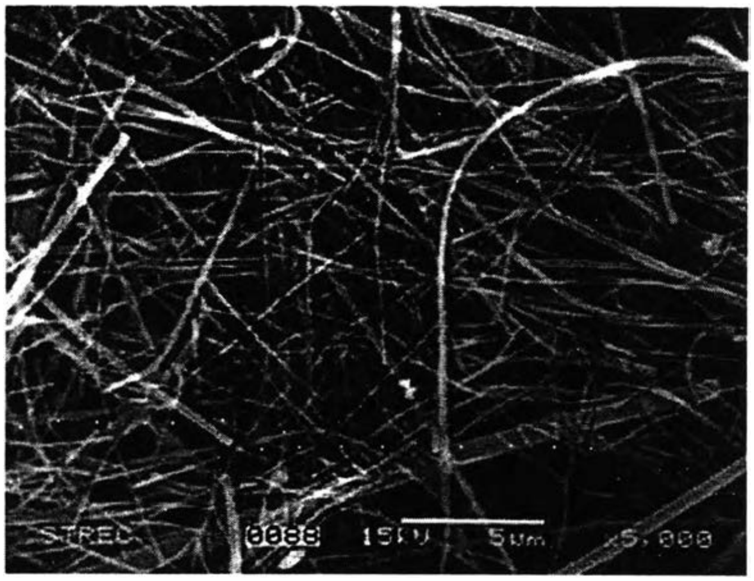

Figure 4.2. SEM image of HEPA filter fibers.

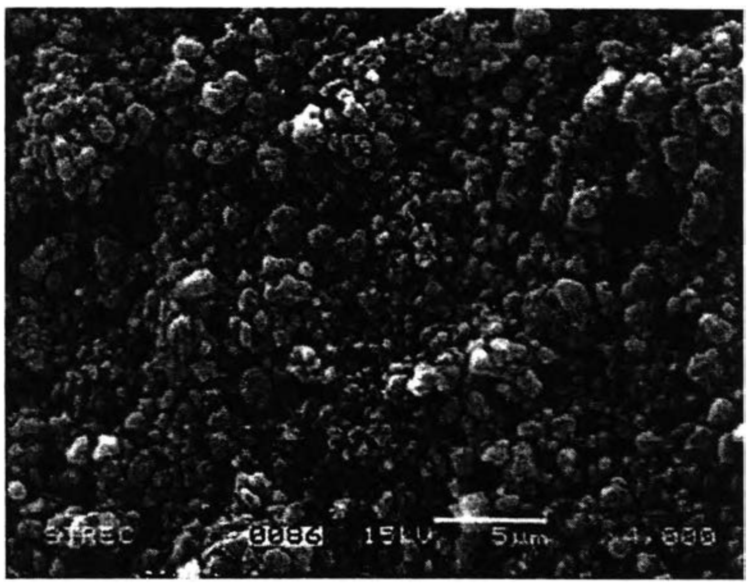

Figure 4.3. SEM image of TiO_2 (T1) cake formed on the surface of HEPA filter.

4.3 Phenol removal using rotary drum filtering photoreactor

In this section, we defined the phenol adsorption, phenol decomposition and TOC depletion efficiencies as given in equations 4.8 - 4.10.

$$\text{Adsorption efficiency (\%)} = (C_0\text{-}C)/C_0 \times 100 \tag{4.8}$$

$$\text{Decomposition efficiency (\%)} = (C_0\text{-}C_{Ir})/C_0 \times 100 \tag{4.9}$$

$$\text{TOC depletion efficiency (\%)} = (TOC_0\text{-}TOC)/TOC_0 \times 100 \tag{4.10}$$

4.3.1 Effect of rotating speed of the drum on phenol removal

Preliminary results on the effect of the rotating speed on the water film thickness on the drum showed that, as the speed increased, the average thickness of the water film on the right side of the drum rotating clockwise became thicker because the time available for the water to filtrate and get sucked into the drum became reduced. In contrast, the water film thickness on the left side of the drum was not much reduced despite the lengthened water sucked-in time because the increased speed enhanced the uplift of left-side water from the water surface in the tank. As a result, the effective average water film thickness became thicker as the rotating speed increased. Table 4.3 lists the initial degradation rate of phenol at various rotating speeds of the drum. In addition, Figs. 4.4 and 4.5 show the experimental results of phenol removal at various rotating speeds of the drum. The decomposition of phenol and TOC depletion decreased when the rotating speed of the drum increased because, as the water film became thicker and its surface rougher, more UV light was absorbed and reflected by the film. Therefore, the rotating speed of the drum affected the phenol removal and the suitable rotating speed of the drum for photocatalytic degradation was 5 rpm, the lowest possible value.

Table 4.3 The initial degradation rate of phenol at various rotating speeds of the drum.

Rotating speed (rpm)	Initial decomposition rate ($mg\ dm^{-3}\ min^{-1}$)	Initial rate of TOC depletion ($mg\ dm^{-3}\ min^{-1}$)
5	0.097	0.039
10	0.021	0.012
20	0.015	0.009
30	0.010	0.007

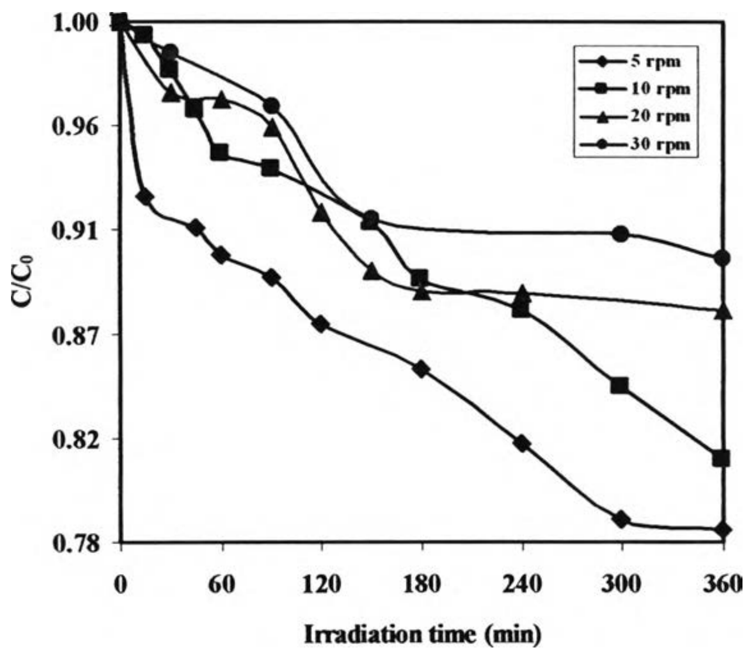

Figure 4.4. Decomposition of phenol at various rotating speeds of the drum using filtration velocity of 0.73 cm min^{-1}.

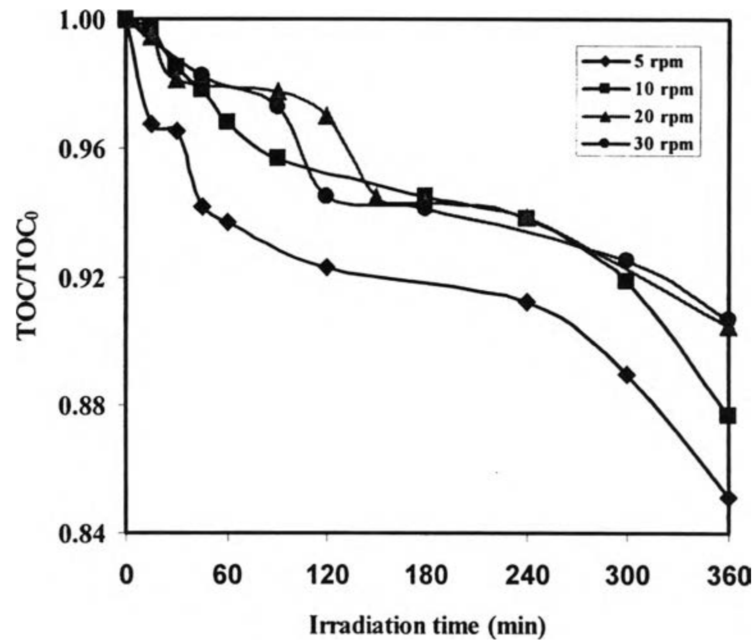

Figure 4.5. TOC depletion at various rotating speeds of the drum using filtration velocity of 0.73 cm min^{-1}.

4.3.2 Effect of filtration velocity on phenol removal

The decomposition of phenol and TOC depletion at various filtration velocities must be studied because it was an important factor of the rotary drum filtering reactor. The rotating speed of 5 and 10 rpm was chosen in studying the effect of filtration velocity on phenol removal and to confirm the effect of the rotating speed of the drum on phenol removal.

The results shown in Figs. 4.6 and 4.7 demonstrated that the phenol removal decreased as the filtration velocity decreased from 0.73 to 0.52 cm min^{-1} since the water film on the drum surface was thicker so the absorption and reflection of UV light by the film was enhanced. For this reason, the photocatalytic degradation in this condition was worse than that at filtration velocity of 0.73 cm min^{-1}. When the filtration velocity increased from 0.73 to 0.84 cm min^{-1}, phenol removal efficiency decreased because the contact time between phenol and titania for photocatalytic degradation became shorter. The suitable filtration velocity in degrading phenol was 0.73 cm min^{-1}. The results could be confirmed experimentally.

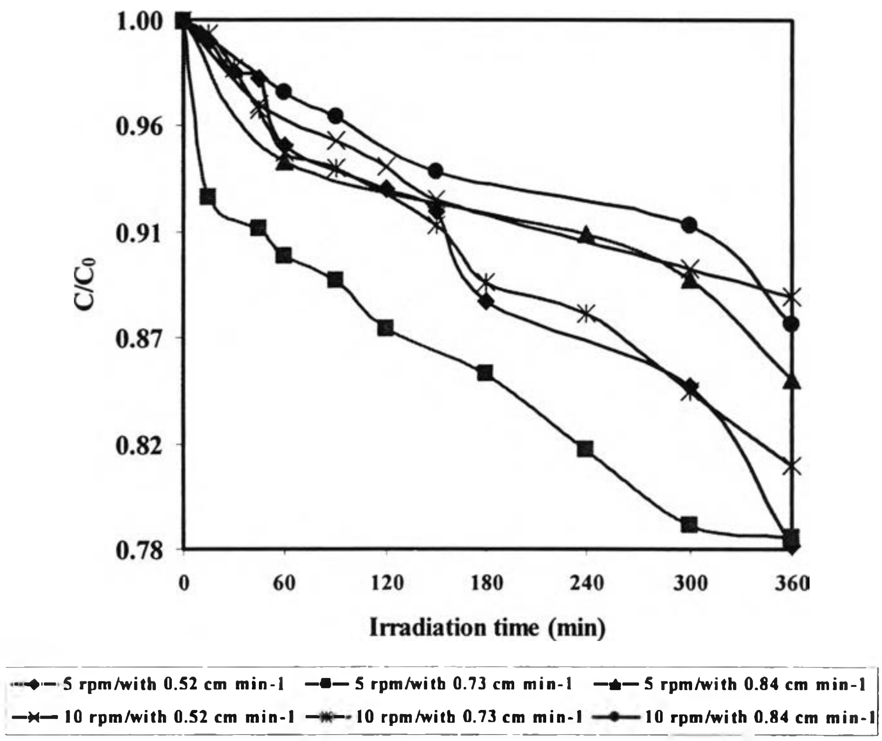

Figure 4.6. Comparison of decomposition of phenol at various filtration velocities.

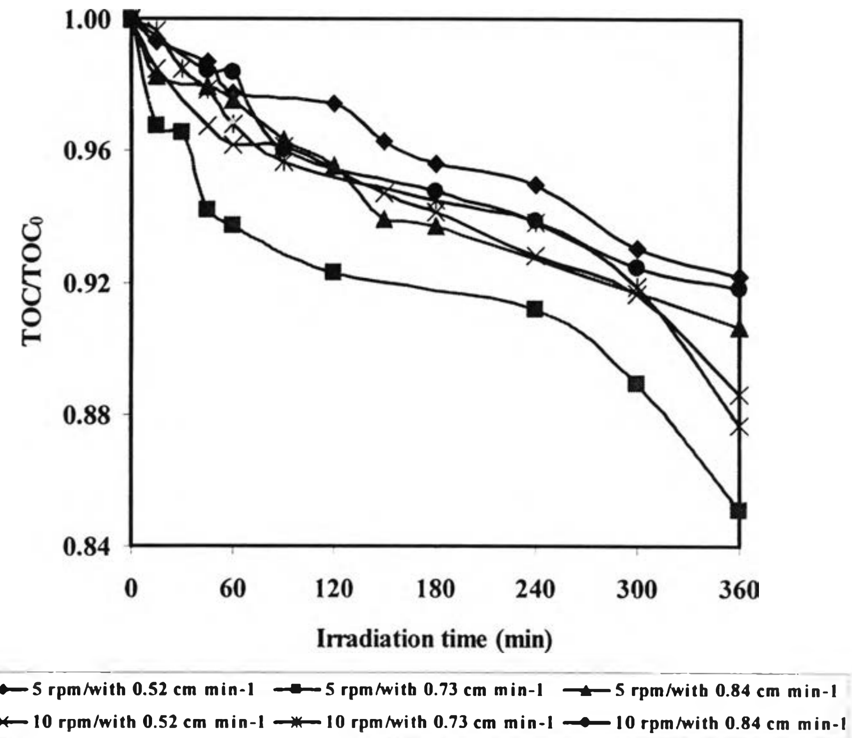

Figure 4.7. Comparison of TOC depletion at various filtration velocities.

4.3.3 Effect of direct photolysis on phenol removal

A direct photolysis experiment was carried out to compare with the performance of TiO_2 cake in degrading phenol. Figs. 4.8 and 4.9 represent the effect of direct photolysis in degrading phenol. Their results indicated that the role of degradation of phenol came from the TiO_2 cake which had the decomposition efficiency of about 20.41 %.

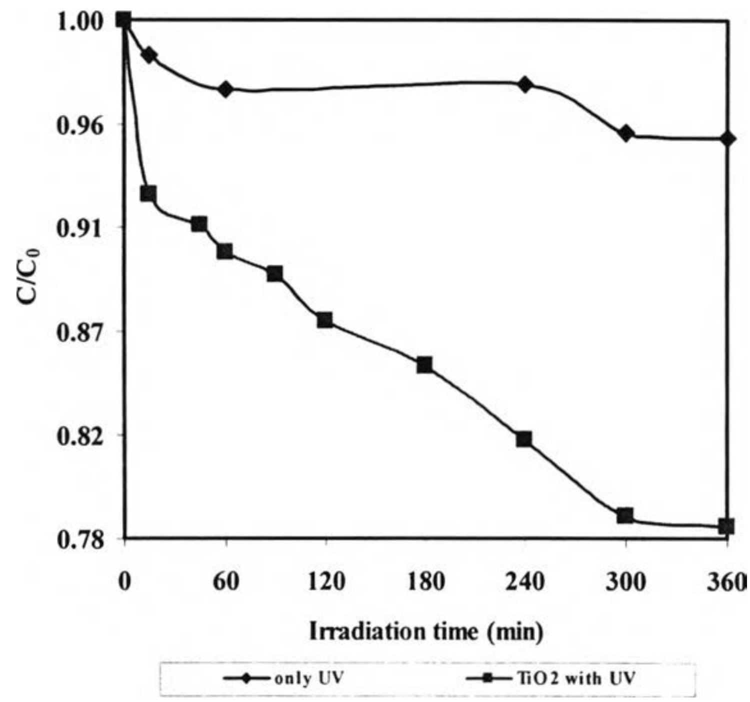

Figure 4.8. Effect of direct photolysis on the decomposition of phenol using rotating speed of the drum of 5 rpm and filtration velocity of 0.73 cm min^{-1}.

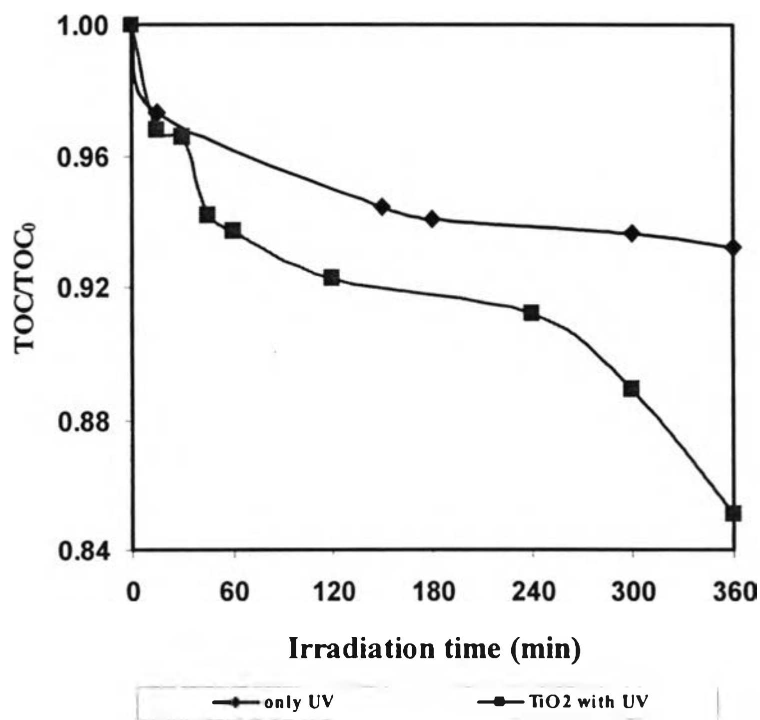

Figure 4.9. Effect of direct photolysis on the TOC depletion using rotating speed of the drum of 5 rpm and filtration velocity of 0.73 cm min^{-1}.

4.3.4 Adsorption of phenol on TiO_2 cake

Dark adsorption experiment was carried out to investigate the adsorption capacity of TiO_2 cake. The results shown in Fig. 4.10 illustrated that the adsorption efficiency of phenol by the TiO_2 cake after 360 min was 7.46 % while it was only 0.95 % after 30 min. In contrast, TiO_2 powder had the batch adsorption capacity of phenol of about 4.21 %, and the adsorption equilibrium was reached within 10 min. Their results indicated that the initial adsorption capacity of the TiO_2 cake was much lower than in the case of TiO_2 powder whereas the long-term adsorption capacity of the TiO_2 cake was higher than in the case of TiO_2 powder.

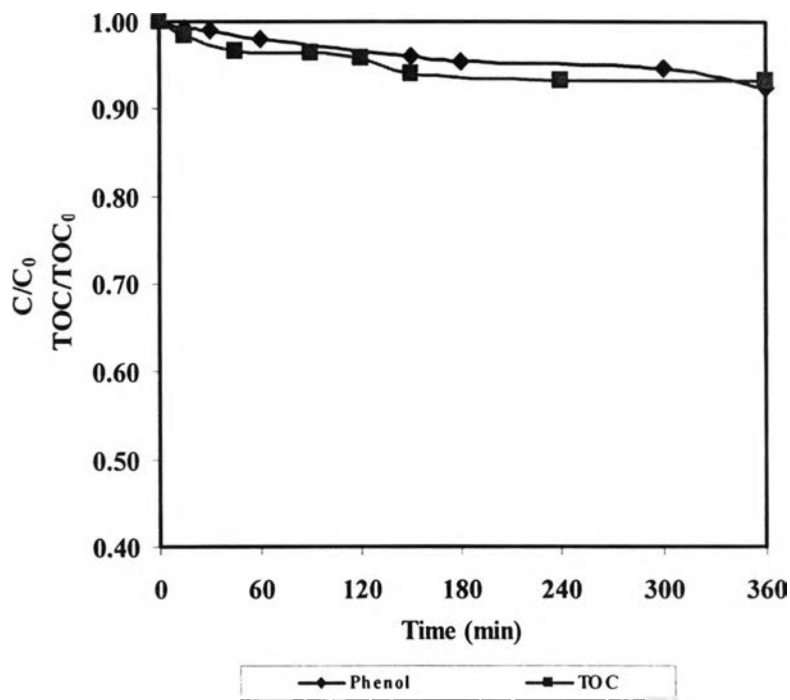

Figure 4.10. Dark adsorption of phenol on TiO_2 cake in terms of phenol and TOC using filtration velocity of 0.73 cm min^{-1} and rotating speed of 5 rpm.